Vol 459|11 June 2009|doi:10.1038/nature08043

LETTERS

Total synthesis of eudesmane terpenes by site-selective C–H oxidations

Ke Chen[1] & Phil S. Baran[1]

From menthol to cholesterol to Taxol, terpenes are a ubiquitous group of molecules (over 55,000 members isolated so far) that have long provided humans with flavours, fragrances, hormones, medicines and even commercial products such as rubber[1]. Although they possess a seemingly endless variety of architectural complexities, the biosynthesis of terpenes often occurs in a unified fashion as a 'two-phase' process[2,3]. In the first phase (the cyclase phase), simple linear hydrocarbon phosphate building blocks are stitched together by means of 'prenyl coupling', followed by enzymatically controlled molecular cyclizations and rearrangements. In the second phase (the oxidase phase), oxidation of alkenes and carbon–hydrogen bonds results in a large array of structural diversity. Although organic chemists have made great progress in developing the logic[3–5] needed for the cyclase phase of terpene synthesis, particularly in the area of polyene cyclizations[6], much remains to be learned if the oxidase phase is to be mimicked in the laboratory. Here we show how the logic of terpene biosynthesis has inspired the highly efficient and stereocontrolled syntheses of five oxidized members of the eudesmane family of terpenes in a modicum of steps by a series of simple carbocycle-forming reactions followed by multiple site-selective inter- and intramolecular carbon–hydrogen oxidations. This work establishes an intellectual framework in which to conceive the laboratory synthesis of other complex terpenes using a 'two-phase' approach.

Synthetic organic chemists have been captivated by terpenes for over 100 years, with the first total syntheses of camphor and terpineol being completed in 1903 and 1904, respectively (ref. 1 and references therein). The origin of terpenes was demystified by the Ruzicka school in 1953 with the formulation of the 'biogenetic isoprene rule' (see refs 7 (last chapter, co-authored with A. Eschenmoser and H. Heusser) and 8). Advances in analytical techniques and the development of retrosynthetic analysis[4] has led to a significant increase in both the number of newly discovered terpenes and the ability to rationally plan and execute their total synthesis[1,3–5]. However, in the case of complex terpenes such as the clinically used anticancer agent paclitaxel, or Taxol (**2**; Fig. 1), the efficiency of biosynthesis is generally far ahead of the current capabilities of chemical synthesis. For example, tonne quantities of 10-deacetyl baccatin III (**3**) are generated annually (presumably via taxadiene (**1**))[9] by the needles of the European yew tree as a fully oxidized renewable starting material for the commercial semi-synthesis of **2** (ref. 10), whereas only milligram quantities of totally synthetic **2** are accessible, and that only with significant effort[1,3]. The lack of general methods, strategies and rules for the functionalization of C–H bonds within complex hydrocarbon systems might account for this difference. Indeed, the total synthesis of multiply oxygenated terpenes using sequential, site-selective C–H functionalizations has not been reported, despite advances in the field of C–H oxidation, specifically for the conversion of a single C–H bond to a C–O bond in diverse settings[11–17]. Here we report such total syntheses using an atypical approach to synthesis design that is inspired by terpene biosynthesis and proceeds in two separate phases (Fig. 1).

The eudesmane family of terpenes (Fig. 1), containing over 1,000 members with almost every conceivable oxidation pattern expressed, was selected for this study[18]. Despite their low molecular weight, the rigid skeleton of these natural products render them difficult targets for synthesis, especially if large quantities are desired. Dihydrojunenol (**4**), one of the lowest oxidized members, has been prepared only once by a stereorandom semi-synthesis from santonin that proceeded in nine steps (8% overall yield) as a separable mixture of three stereoisomers[19]. An elegant enantioselective total synthesis of eudesmanes similar in complexity to **4** proceeded in 15 steps (milligram quantities, 14% overall yield)[20]. Related family members that have not been previously synthesized are 4-epiajanol (**5**)[21] dihydroxyeudesmane (**6**)[22], pygmol (**7**)[23] and eudesmantetraol (**8**)[24]; these were thought to arise from **4**. A robust and simple route to **4** (the equivalent of a cyclase phase) would set the stage for site-selective oxidations of two of its five tertiary C–H bonds to access **5**–**8** (the equivalent of an oxidase phase).

The gram-scale preparation of **4** (Fig. 2) involved a nine-step sequence, five steps of which generated C–C bonds and four of which set key stereocentres. Thus, an enantioselective intermolecular Michael reaction of 3-methyl butyraldehyde and methyl vinyl ketone, catalysed by prolinol **9** (refs 25, 26), followed by treatment with base, led to formation of the natural product cryptone (**10**) in 63% overall yield and 89% enantiomeric excess. The route to this simple terpene is superior in terms of step count and overall yield to a dozen previously reported syntheses (see Supplementary Information for references). Iodination of **10** proceeded in nearly quantitative yield to afford the iodoenone **11**. Introduction of the side chain by Grignard addition and subsequent 1,3-carbonyl transposition furnished intermediate **12** (74% overall yield). The decalin framework of the eudesmanes was forged using an intramolecular Heck cyclization under standard conditions to deliver diene **13** in 95% yield. The final carbon atom was installed by a regio- and stereoselective 1,4-addition and tandem isomerization to afford enone **14** in 56% yield (along with recovered **13**). A two-step strategic reduction sequence set the three consecutive steric centres of **4** in 87% overall yield as a single diastereomer. By this route, gram quantities of enantiopure **4** were prepared (21% overall yield).

With ample quantities of **4** available, a systematic exploration of oxidation chemistry could take place (Fig. 3). Our studies were influenced by those of Chen and White, who were the first to explicitly demonstrate that steric and electronic factors can be used to predict the selectivity of intermolecular tertiary C–H oxidation in complex settings using iron catalysis[17]. To begin, the trifluoroethyl carbamate directing group[27] was installed in quantitative yield to deliver **15**. This group served the purpose of depleting electron density from the neighbouring carbon atoms (deactivating them against electrophilic

[1]Department of Chemistry, The Scripps Research Institute, 10550 N. Torrey Pines Road, La Jolla, California 92037, USA.

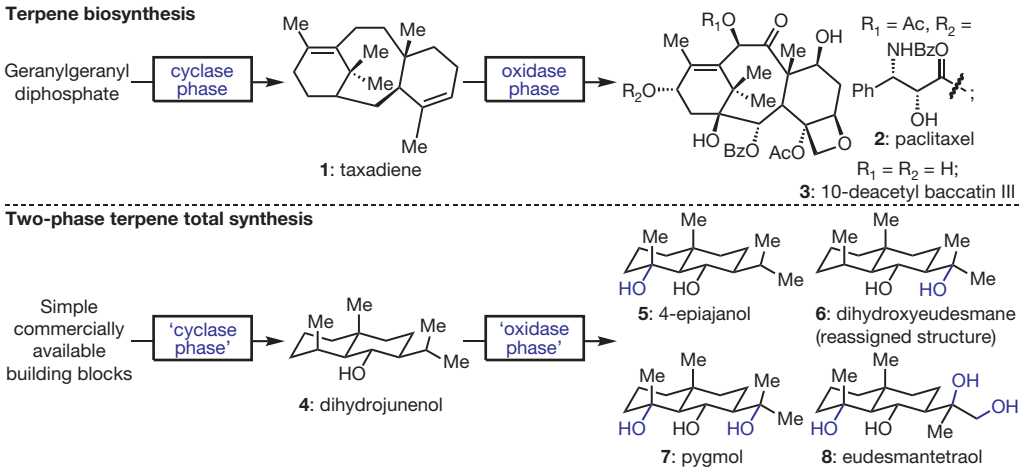

Figure 1 | Outline of the 'two-phase' approach to terpene total synthesis. Me, methyl; Ac, acetyl; Bz, benzoyl.

attack) and would be used to direct other crucial transformations. A C–H bond reactivity analysis using X-ray crystallography and ^{13}C nuclear magnetic resonance (NMR) allowed for a qualitative differentiation of the five tertiary C–H bonds in structure **15**, H_1–H_5. Using ^{13}C NMR chemical shifts (δ), the relative electronegativity trend for the tertiary carbon atoms was established as follows:

$$\delta_{C3} = 73.6 \text{ p.p.m.} > \delta_{C2} = 55.2 \text{ p.p.m.} \approx \delta_{C4} = 50.2 \text{ p.p.m.} > \delta_{C1} = 27.5 \text{ p.p.m.} \approx \delta_{C5} = 26.6 \text{ p.p.m.}$$

This implies that H_1 and H_5 are the most likely tertiary C–H bonds to be oxidized with an electrophilic oxidant. Furthermore, X-ray crystallography and modelling studies suggest that H_1 adopts an equatorial orientation and that H_5 is populated by multiple conformers. The studies of Curci[11] demonstrated that powerful organic oxidants such as dioxiranes selectively oxidize equatorially oriented C–H bonds in preference to those adopting an axial configuration.

In the event, site-specific intermolecular oxidation of carbamate **15** using TFDO (1.0 equiv.) led to the formation of intermediate **16** in 82% isolated yield on a gram scale (Fig. 3). The origin of this selectivity may stem from strain-release effects in the transition state during oxidation[28], a subject to be examined in future investigations. Basic hydrolysis of **16** led to 4-epiajanol (**5**) and its structure was verified by X-ray crystallography[21]. Consistent with the electronic rules set forth by White and Chen[17], substrate **15** did not incur substantial levels of oxidation at either H_1 or H_5 using Fe-based catalysis. To oxidize H_5 first without disturbing H_1, the trifluoroethyl carbamate directing group was exploited because geometric constraints (as judged from molecular models) prevent this directing group from reaching H_1. Using our previously reported conditions[27], site-specific halogenation of **15** to **17** was accomplished followed by cyclization and hydrolysis to afford a compound (**6**) that exhibited spectroscopic measurements identical to those reported for dihydroxyeudesmane (**6′**)[22]. The originally assigned structure (**6′**) must therefore be reassigned as depicted for **6** (verified by X-ray crystallography).

To access the higher oxidation states of this family (Fig. 4), which contain three or four hydroxyl groups, **16** was oxidized to bromide **18** by using our previously reported conditions to achieve site-specific halogenation. Silver-assisted cyclization to carbonate **19** and hydrolysis afforded natural product pygmol (**7**). This sequence (52% isolated yield in addition to 30% recovered **16**) was carried out in two separate vessels and could be intercepted at the crystalline carbonate **19** to verify the structure by X-ray crystallography. The tetrahydroxylated natural product eudesmantetraol (**8**) was accessed by a formal remote dehydrogenation process. Thus, the tertiary bromide in **18** was eliminated with tetramethylpiperidine to afford an intermediate alkene (**20**). The

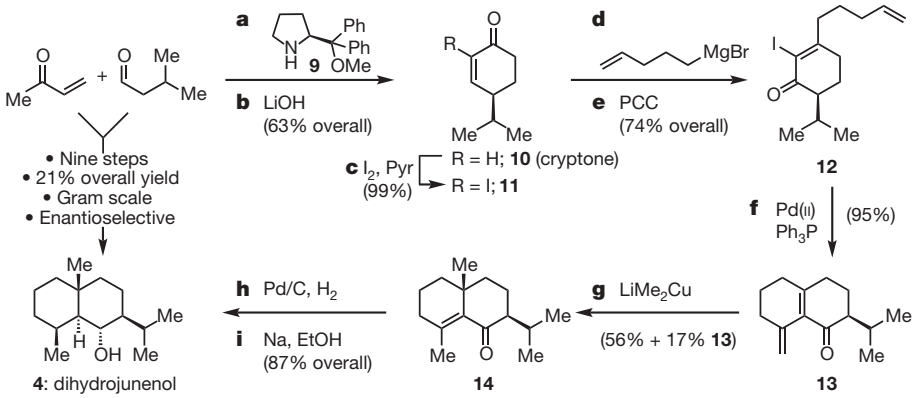

Figure 2 | Simple, enantioselective total synthesis of dihydrojunenol (4). Reagents and conditions as follows. **a**, Methyl vinyl ketone (1.5 equiv.), 3-methyl butyraldehyde (1.0 equiv.), prolinol catalyst (0.05 equiv.), ethyl 3,4-dihydroxybenzoate (0.20 equiv.), neat, 4 °C, 36 h, 89%. **b**, LiOH (0.1 equiv.), *i*-PrOH, room temperature (RT, 23 °C), 24 h, 63% over two steps, 89% enantiomeric excess. **c**, I_2 (1.2 equiv.), Pyr/DCM, RT, 12 h, 99%. **d**, $(CH_2CHCH_2CH_2CH_2)MgBr$ (1.5 equiv.), toluene, −78 °C, 30 min; then 0 °C, 30 min. **e**, PCC (1.2 equiv.), 3 Å MS, DCM, RT, 6 h, 74% over two steps. **f**, $Pd(OAc)_2$ (0.1 equiv.), Ph_3P (0.3 equiv.), Et_3N (1.2 equiv.), Ag_2CO_3 (1.0 equiv.), CH_3CN, 70 °C, 3 h, 95%. **g**, $LiMe_2Cu$ (1.5 equiv.), DCM, 0 °C, 4 h, 56% (17% recovered starting material). **h**, H_2 (1 atm), Pd/C (0.1 equiv.), EtOAc, RT, 30 min. **i**, Na (5 equiv.), EtOH, RT, 30 min, 87% over two steps. Et_3N, triethylamine; DCM, dichloromethane; I_2, iodine; Pyr, pyridine; PCC, pyridinium chlorochromate; MS, molecular sieves; Ph_3P, triphenylphosphine; CH_3CN, acetonitrile; $LiMe_2Cu$, lithium dimethylcuprate; EtOAc, ethyl acetate. For selected physical data for compounds **11**, **12**, **13**, **14** and **4**, see the Supplementary Information.

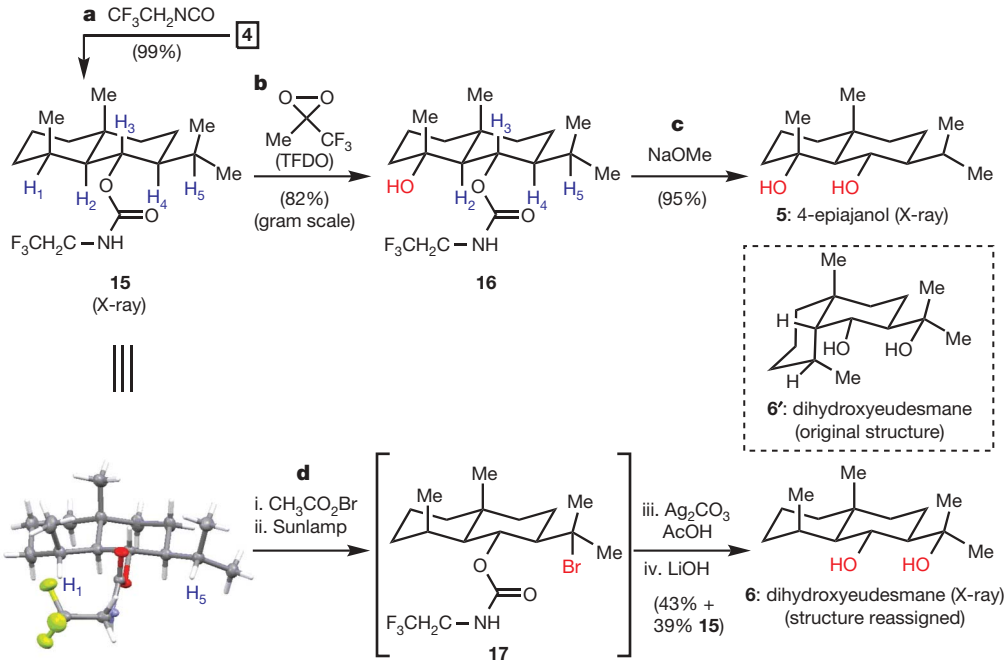

Figure 3 | Total syntheses of 4-epiajanol (5) and dihydroxyeudesmane (6) through site-specific C–H oxidations of dihydrojunenol (4). Reagents and conditions as follows. **a**, CF_3CH_2NCO (1.0 equiv.), Pyr (4.0 equiv.), DMAP (catalytic), DCM, RT, 1 h, 99%. **b**, TFDO (1.0 equiv.), DCM, −20 °C, portion-wise addition of TFDO over 30 min, then additional 30 min, 82%. **c**, NaOMe (5.0 equiv.), MeOH, 70 °C, 2 h, 95%. **d**, CH_3CO_2Br (1.0 equiv.), DCM, 0 °C, 5 min; $PhCF_3$, 100-W sunlamp, 10 min; Ag_2CO_3 (1.2 equiv.), DCM, RT, 30 min, then aqueous acetic acid, RT, 30 min; LiOH (10 equiv.), THF/H_2O, RT, 10 min, 43% (39% recovered **15**). DMAP, 4-dimethylaminopyridine; TFDO, methyl(trifluoromethyl)dioxirane; NaOMe, sodium methoxide; THF, tetrahydrofuran. For selected physical data for compounds **5**, **6**, **15** and **16**, see the Supplementary Information. Compounds **5**, **6** and **15** were verified by X-ray crystallography.

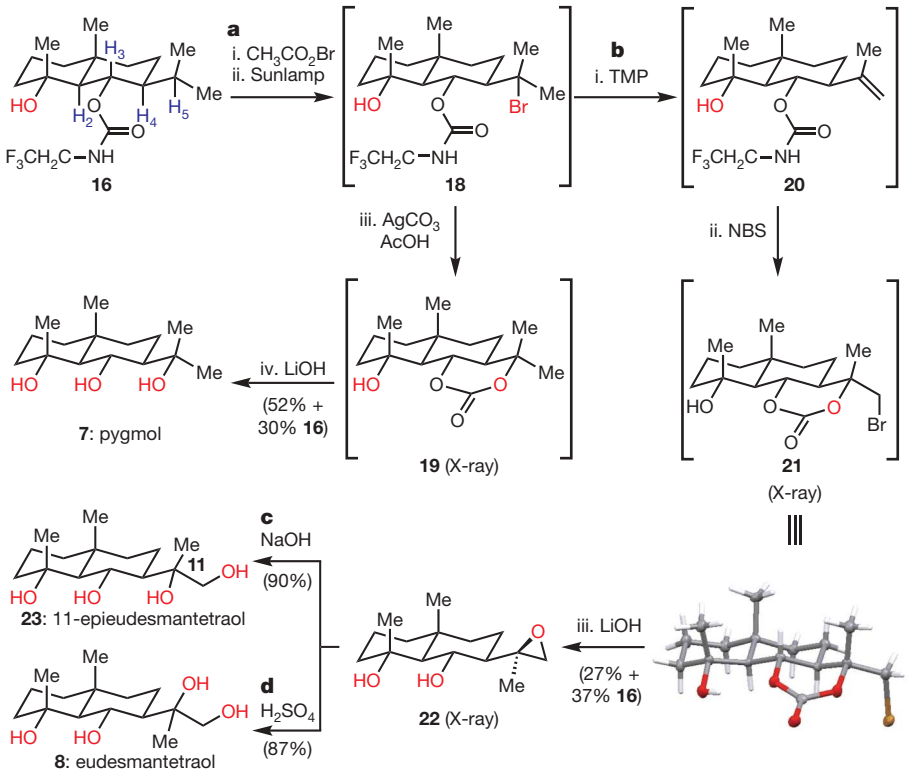

Figure 4 | Total syntheses of pygmol (7) and eudesmantetraol (8) through site-specific C–H oxidations of 16. Reagents and conditions as follows. **a**, CH_3CO_2Br (1.0 equiv.), DCM, 0 °C, 5 min; $PhCF_3$, 100-W sunlamp, 20 min; Ag_2CO_3 (1.2 equiv.), DCM, RT, 30 min, then aqueous acetic acid, RT, 30 min; LiOH (10 equiv.), THF/H_2O, RT, 10 min, 52% (30% recovered **16**). **b**, TMP (2.0 equiv.), toluene, 80 °C, 12 h; NBS (2.0 equiv.), DCM, RT, 6 h, then aqueous acetic acid, RT, 30 min; LiOH (10 equiv.), THF/H_2O, RT, 10 min, 27% (37% recovered **16**). **c**, 3 M NaOH, DMSO, 80 °C, 2 h, 90%. **d**, 0.1 M H_2SO_4, DME/H_2O, RT, 1 h, 87%. TMP, 2,2,6,6-tetramethylpiperidine; NBS, *N*-bromosuccinimide; DMSO, dimethylsulphoxide; DME, 1,2-dimethoxyethane. For selected physical data for compounds **7**, **8**, **19**, **21**, **22** and **23**, see the Supplementary Information. Compounds **19**, **21** and **22** were verified by X-ray crystallography.

neighbouring trifluoroethyl carbamate could be cyclized onto this alkene using NBS to afford the bromocarbonate **21** (structure verified by X-ray crystallography) as a single diastereomer. This two-step sequence represents a rare example of carbamate-directed remote dehydrogenation and the use of a carbamate to achieve intramolecular stereocontrolled oxybromination of an alkene. Treatment with LiOH led to epoxide intermediate **22** (structure verified by X-ray crystallography) in 27% overall isolated yield (the C–H activation step proceeds in ~60% isolated yield) for the three-step sequence. Exposure of **22** to NaOH furnished 11-epieudesmantetraol **23** with retention of stereochemistry (90% yield), whereas treatment with dilute acid afforded eudesmantetraol (**8**) as a single diastereomer in 87% yield by net inversion. Notably, the dihydroxylation of olefin **20** using OsO_4 was not stereoselective, giving a mixture of diol products (Sharpless AD-mixes were also ineffective).

As such, the terpenes cryptone (**10**), dihydrojunenol (**4**), 4-epiajanol (**5**), dihydroxyeudesmane (**6**), pygmol (**7**) and eudesmantetraol (**8**) were respectively constructed in 2, 9, 12, 12, 13 and 15 steps and in 63, 21, 17, 9, 9 and 4% overall isolated yield from two feedstock carbon sources (methyl vinyl ketone and 3-methyl butyraldehyde) without any recycling of recovered starting materials. Before this work, a single late-stage C–H-to-C–OH conversion was used for the diversification of bryostatin analogues[14], the semi-synthesis of various natural products such as steroids[16] and artemisinin[17], and the preparation of linear (E)-allylic alcohols[29]. This work presents an example of a linear C–H activation strategy featuring multiple consecutive site-selective oxidations in total synthesis.

The straightforward logic employed in this atypical approach to terpene synthesis begins with the construction of a 'retrosynthesis pyramid' diagram as shown in Fig. 5. The retrosynthesis pyramid places the highest oxidized target at the apex and works backward until the lowest oxidized members are reached. Rather than making strategic disconnections to a single molecule, multiple molecules are considered at every descending level of oxidation. Next, each individual level of 'redox isomers' is scrutinized for feasibility in the required oxidation to reach the next level. By analysing several molecules with equivalent overall oxidation state, there is no limitation to a certain oxidation reaction (that is, the conversion of C–H to C–X or direct dehydrogenation to an alkene can sometimes be more strategic than the conversion of C–H to C–O). It is here that issues of choreography, reaction methodology and chemoselectivity are evaluated. On reaching the lowest oxidation level, a final target is chosen for both its ease of synthesis and its potential to access the greatest number of possible intermediates as the pyramid is ascended. Because much of the chemistry necessary to reach the apex may be poorly precedented and require reaction invention, it is critical that the starting material be available in large (gram-scale) quantities. After the planning necessary to mimic the oxidase-phase has been concluded, the most logical starting material can then be evaluated using standard retrosynthetic analysis (this is the conceptual equivalent to the cyclase phase in biosynthesis). A detailed discussion of the implementation of the retrosynthesis pyramid for this work is contained in the Supplementary Information.

One of the main characteristics of terpene biosynthesis is that installation of functional groups (oxidation) onto the carbon framework usually occurs near the end of the sequence (a notable exception being the oxidation of squalene to squalene oxide[6–8]). These syntheses demonstrate that there may be certain advantages to conducting terpene synthesis in a similar manner. Because most of the heteroatoms are installed at the end of the synthesis, chemoselectivity becomes less of a concern during the early stages[29]. This also leads to a minimization of protecting group chemistry during the cyclase phase and allows for a greater variety of chemistry to be employed with less

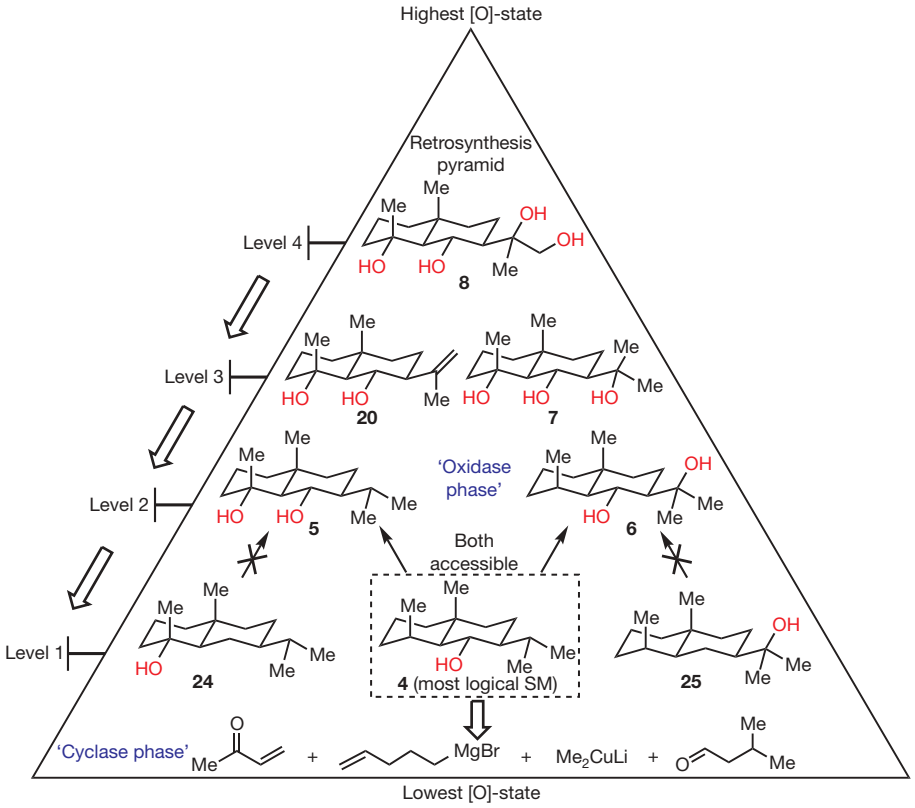

Figure 5 | Pyramid diagram for the retrosynthetic planning of terpene synthesis using a 'two-phase' approach. Because eudesmantetraol (**8**) is the highest oxidized target, it is placed at the apex. Removal of one hydroxyl group leads to level-3 intermediates **20** and **7** (and any synthetic equivalents such as an alkyl bromide, for example **18** in Fig. 4). Repetition of this transform leads to diols **5** and **6** (level 2), either of which could conceivably access **20** or **7**. Subsequent deoxygenation of these level-2 intermediates leads to three selections for level 1: **24**, **4** and **25**. Dihydrojunenol (**4**) was chosen as the most logical starting material owing to its potential to access both **5** and **6** without any corrective reduction steps or a difficult C–H activation of a methylene group. [O]-state, oxidation state; SM, starting material.

concern for side reactions. Additionally, this biomimetic approach can naturally lead to the synthesis of related family members, closely related analogues (for example **5** and **23**) and in some cases even structural reassignments (for example **6′** → **6**). Finally, the use of a retrosynthesis pyramid when planning the oxidase phase can encourage the invention of useful methodology and greater insight into the relative reactivity of different tertiary C–H bonds.

This work represents another[11–17,30] step towards the generation of a set of rules and logic for the use of C–H oxidation in terpene synthesis. Whether or not elements of such a strategy could be employed in the synthesis of terpenes at the highest level of complexity (for example **2**; Fig. 1) remains to be seen. There are obvious limitations in current synthetic methodology that will need to be overcome for the logic of this approach to reach its full potential, such as the oxidation of primary and secondary C–H bonds in a controllable manner, a broader functional group tolerance and more general, high-yielding protocols for C–H oxidation. Finally, we note that the use of a trifluoroethyl carbamate directing group is both an advantage and a limitation. Its use permitted site-selective oxidations of both sp^3-hybridized (**15** to **17** and **16** to **18**) and sp^2-hybridized (**20** to **21**) carbon atoms that would have been difficult to achieve in an intermolecular fashion with currently available reagents. Furthermore, it shielded the reactivity of a secondary alcohol, allowing intermolecular C–H oxidation (**15** to **16**) and rendering several intermediates crystalline for X-ray characterization purposes. Conversely, its installation requires an additional step and this points to two directions for future attempts to imitate the oxidase phase of terpene biosynthesis: site-specific C–H oxidation without any directing groups and reagent-dependent reordering of C–H bond reactivity.

METHODS SUMMARY

All reactions were carried out under a nitrogen atmosphere with dry solvents under anhydrous conditions, unless otherwise noted. Yields refer to chromatographically and spectroscopically homogeneous materials, unless otherwise stated. Reagents were purchased at the highest commercial quality and used without further purification, unless otherwise stated. Reactions were monitored using thin-layer chromatography. For full experimental details and procedures for all reactions performed and full characterization (^{1}H NMR, ^{13}C NMR, high-resolution mass spectrometry, infrared, optical rotation, melting point and R_f value) of all new compounds, see Supplementary Information.

Received 17 February; accepted 7 April 2009.
Published online 13 May 2009.

1. Nicolaou, K. C. & Montagnon, T. *Molecules That Changed the World* (Wiley-VCH, 2008).
2. Davis, E. M. & Croteau, R. Cyclization enzymes in the biosynthesis of monoterpenes, sesquiterpenes and diterpenes. *Top. Curr. Chem.* **209,** 53–95 (2000).
3. Maimone, T. J. & Baran, P. S. Modern synthetic efforts toward biologically active terpenes. *Nature Chem. Biol.* **3,** 396–407 (2007).
4. Corey, E. J. & Cheng, X. M. *The Logic of Chemical Synthesis* (Wiley, 1995).
5. Wilson, R. & Danishefsky, S. J. Pattern recognition in retrosynthetic analysis: snapshots in total synthesis. *J. Org. Chem.* **72,** 4293–4305 (2007).
6. Yoder, R. A. & Johnston, J. N. A case study in biomimetic total synthesis: polyolefin carbocyclizations to terpenes and steroids. *Chem. Rev.* **105,** 4730–4756 (2005).
7. Ruzicka, L. Isoprene rule and the biogenesis of terpenic compounds. *Experentia* **9,** 357–367 (1953).
8. Eschenmoser, A. & Arigoni, D. Revisited after 50 years: the 'Stereochemical interpretation of the biogenetic isoprene rule for the triterpenes'. *Helv. Chim. Acta* **88,** 3011–3050 (2005).
9. Jennewein, S., Rithner, C. D., Williams, R. M. & Croteau, R. B. Taxol biosynthesis: taxane 13α-hydroxylase is a cytochrome P450-dependent monooxygenase. *Proc. Natl Acad. Sci. USA* **98,** 13595–13600 (2001).
10. Denis, J. N. *et al.* Highly efficient, practical approach to natural Taxol. *J. Am. Chem. Soc.* **110,** 5917–5919 (1988).
11. Mello, R., Fiorentino, M., Fusco, C. & Curci, R. Oxidations by methyl(trifluoromethyl)dioxirane. 2. Oxyfunctionalization of saturated hydrocarbons. *J. Am. Chem. Soc.* **111,** 6749–6757 (1989).
12. Costas, M., Mehn, M. P., Jensen, M. P. & Que, L. Jr. Dioxygen activation at mononuclear nonheme iron active sites: enzymes, models, and intermediates. *Chem. Rev.* **104,** 939–986 (2004).
13. Groves, J. T., Bonchio, M., Carofiglio, T., &. Shalyaev, K. Rapid catalytic oxygenation of hydrocarbons by ruthenium pentafluorophenylporphyrin complexes: evidence for the involvement of a Ru(III) intermediate. *J. Am. Chem. Soc.* **118,** 8961–8962 (1996).
14. Wender, P. A., Hilinski, M. K. & Mayweg, A. V. W. Late-stage intermolecular C-H activation for lead diversification: a highly chemoselective oxyfunctionalization of the C-9 position of potent bryostatin analogues. *Org. Lett.* **7,** 79–82 (2005).
15. Brodsky, B. H. & Du Bois, J. Oxaziridine-mediated catalytic hydroxylation of unactivated 3° C–H bonds using hydrogen peroxide. *J. Am. Chem. Soc.* **127,** 15391–15393 (2005).
16. Yang, J., Gabriele, B., Belvedere, S., Huang, Y. & Breslow, R. Catalytic oxidations of steroid substrates by artificial cytochrome P-450 enzymes. *J. Org. Chem.* **67,** 5057–5067 (2002).
17. Chen, M. S. & White, M. C. A predictably selective aliphatic C-H oxidation reaction for complex molecule synthesis. *Science* **318,** 783–787 (2007).
18. Wu, Q.-X., Shi, Y.-P. & Jia, Z.-J. Eudesmane sesquiterpenoids from the Asteraceae family. *Nat. Prod. Rep.* **23,** 699–734 (2006).
19. Cardona, L., Garcia, B., Gimenez, E. & Pedro, J. R. A shorter route to the synthesis of (+)-junenol, isojunenol, and their coumarate esters from (−)-santonin. *Tetrahedron* **48,** 851–860 (1992).
20. Levine, S. R., Krout, M. R. & Stoltz, B. M. Catalytic enantioselective approach to the eudesmane sesquiterpenoids: total synthesis of (+)-carissone. *Org. Lett.* **11,** 289–292 (2009).
21. Paknikar, S. K., Dhekne, V. V. & Joshi, G. D. Synthesis of 4α, 6α-dihydroxyeudesmane: revision of stereochemistry at C-4 of ajanol. *Indian J. Chem.* **15B,** 86–87 (1977).
22. Zhao, P.-J., Li, G.-H. & Shen, Y.-M. New chemical constituents from the endophyte Streptomyces species LR4612 cultivated on Maytenus hookeri. *Chem. Biodivers.* **3,** 337–342 (2006).
23. Irwin, M. A. & Geissman, T. A. Sesquiterpene alcohols from *Artemisia pygmaea*. *Phytochemistry* **12,** 849–852 (1973).
24. De Marino, S. *et al.* New sesquiterpene lactones from *Laurus nobilis* leaves as inhibitors of nitric oxide production. *Planta Med.* **71,** 706–710 (2005).
25. Betancort, J. M. & Barbas, C. F. Catalytic direct asymmetric Michael reactions: taming naked aldehyde donors. *Org. Lett.* **3,** 3737–3740 (2001).
26. Chi, Y. & Gellman, S. H. Diphenylprolinol methyl ether: a highly enantioselective catalyst for Michael addition of aldehydes to simple enones. *Org. Lett.* **7,** 4253–4256 (2005).
27. Chen, K., Richter, J. M. & Baran, P. S. 1,3-diol synthesis via controlled, radical-mediated C-H functionalization. *J. Am. Chem. Soc.* **130,** 7247–7249 (2008).
28. Schreiber, J. & Eschenmoser, A. Über die relative Geschwindigkeit der Chromosäureoxydation sekundärer, alicyclischer Alkohole. Vorläufige Mitteilung. *Helv. Chim. Acta* **38,** 1529–1536 (1955).
29. Fraunhoffer, K. J., Bachovchin, D. A. & White, M. C. Hydrocarbon oxidation vs C−C bond-forming approaches for efficient syntheses of oxygenated molecules. *Org. Lett.* **7,** 223–226 (2005).
30. Davies, H. M. L. & Manning, J. R. Catalytic C–H functionalization by metal carbenoid and nitrenoid insertion. *Nature* **451,** 417–424 (2008).

Supplementary Information is linked to the online version of the paper at www.nature.com/nature.

Acknowledgements We are grateful to A. Eschenmoser for discussions and to Bristol-Myers Squibb for financial support. M. Morón Galán and Y. Ishihara are acknowledged for technical contributions to the early stages of this project. We are grateful to B. Shi and A. Reingold for assistance with high-performance liquid chromatography and X-ray crystallographic analyses, respectively.

Author Information The X-ray crystallographic coordinates for the structures reported in this paper have been deposited at the Cambridge Crystallographic Data Centre, under deposition numbers CCDC 718278 (**5**), CCDC 719000 (**6**), CCDC 718279 (**15**), CCDC 718280 (**19**), CCDC 718281 (**21**) and CCDC 718282 (**22**). These data can be obtained free of charge from the Cambridge Crystallographic Data Centre (http://www.ccdc.cam.ac.uk/data_request/cif). Reprints and permissions information is available at www.nature.com/reprints. Correspondence and requests for materials should be addressed to P.S.B. (pbaran@scripps.edu).